AEROELASTICITY OF SLENDER PLEXIGLASS FACADES

Alexander Tesár*

Assessment of ultimate aeroelastic response of slender facades equipped with thin plexiglass sheets. The wave approach is used for modeling of aeroelastic wind forcing. The analysis of structural response is based on the transient dynamics. Some theoretical approaches are specified with experimental verification in the wind canal. The comparison of numerical and experimental approaches is made in order to demonstrate the efficiency of the procedures suggested.

Keywords : *aeroelasticity, equations of motion, frequency domain, laminar and turbulent air flow, plexiglass sheet, slender facades, transient dynamics, wave approach, wind canal*

1. Introduction

The development of suitable techniques for the assessment of ultimate aeroelastic behaviour of slender facade walls equipped with thin glass or plexiglass sheets is the focus of efforts in present paper (Figs. 1 and 2). Sophisticated aeroelastic analysis is required in order to answer the questions associated with reliability of such structures.

Slender facades of above type are prone to wind induced vibrations for various reasons. Some of the issues considered in their wind resistant design are mentioned as follows :

1. Wind turbulences force the facade with a considerable power. The forced movements and sound effects owing to turbulences and associated mechanisms are stochastic in nature.
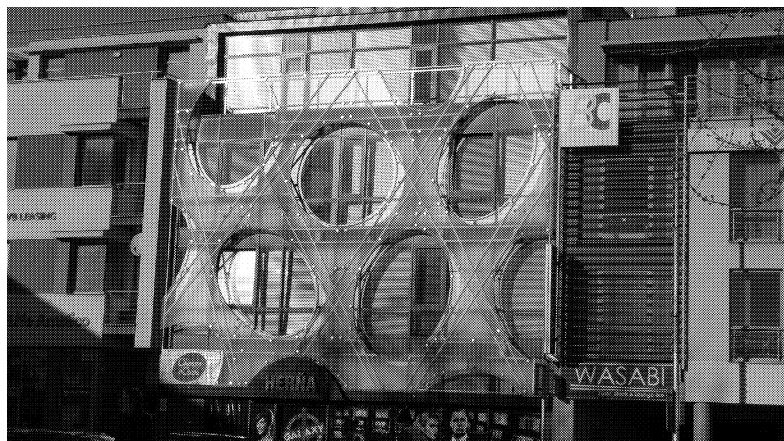

Fig.1: Cheese House in Nitra, Slovakia

* doc. Ing. A. Tesár, DrSc., Institute of Construction and Architecture, Slovak Academy of Sciences, Dubravska cesta 9, 845 03 Bratislava 45, Slovak Republic

Fig.2: Cheese House in Nitra, Slovakia – detailed view

2. Slender facade sheet can produce a strong vortex wake associated with aerodynamic drag force. Depending on the wind speed and geometry of the sheet, the shedding of vortices is more or less regular with shedding periods inversely proportional to the wind speed. In resonant conditions the structure's oscillation can control the rhythm of the vortex shedding and limited amplitude vibrations occur. However, aside the known vortex trail type excitation the more general types of aerodynamic forcing can appear there. The possible re- attachement of separated flow, the vortices generated by the local geometry and by the movement of the facade sheet contribute to aerodynamic forces and induced sounds experienced by the structure.

3. Aerodynamic forces proportional to such movement can produce self-induced divergent vibrations at high wind speeds. In theoretical treatment the concepts of aerodynamic damping and aerodynamic stiffness are applied frequently. In the design is to be avoided that absolute value of negative aerodynamic damping exceeds the damping force producing oscillatory torsional or across-wind flexural mode instability. Associated critical wind speed is the flutter velocity and corresponding circular frequency is termed as flutter frequency of structure.

4. At the onset of divergence the aerodynamic instability of structure can be initiated.

In this paper the wind induced structural phenomena are treated by transient dynamics. The aeroelastic forcing is studied adopting the wave propagation approach. The goal is to develop the approach based on combined transient dynamics versus forcing wave propagation for the assessment of ultimate aeroelastic response of slender facade sheets.

In order to manage the problem 'garbage in, garbage out' in the analysis, the strategy suggested works with the databasis of input data obtained by experimental tests in the wind canal. Such databasis is adopted for virtual assessment of the problem.

2. Analysis of aeroelastic phenomena

The time and frequency domains are two frequently used approaches for aeroelastic assessment of the facade sheets studied. For the loads changing in time the first approach leads to convolution type time integrals, while the second one adopts the Fourier transformed equations of motion with the frequency as fundamental parameter. For the specification

of aeroelastic loads in time domain the indicial aerodynamic functions are applied. The choice of method is complementary, because the flutter derivatives and indicial aerodynamic functions perform the Fourier transform relationships between each other. The wind canal tests of the scale models are to be carried out in order to specify such aeroelastic forcing.

In scope of the spectral analysis the frequency-domain method is applied to the problems, where the statistical properties of turbulences are given by frequency dependent spectral densities and coherence functions. The advantages of the frequency domain method for modeling of aeroelastic action of the facade sheets are obvious. The flutter derivatives appearing are the functions of frequency of vibration and are directly applied to the Fourier-transformed equations of motion. The adoption of flutter derivatives in time domain is restricted to harmonic motion only, while in frequency domain they hold for the analysis of an arbitrary motion. The Fourier-transformed equations of motion are given by

$$(-\omega^2\,\mathbf{M} + \mathrm{i}\,\omega\,\mathbf{C} + \mathbf{K})\,\mathbf{X}(\omega) = [\mathrm{i}\,\omega\,\mathbf{C}_{\mathrm{Ae}}(\omega) + \mathbf{K}_{\mathrm{Ae}}(\omega)]\,\mathbf{X}(\omega) + \mathbf{F}_{\mathrm{b}}(\omega)\;, \tag{1}$$

where ω is the circular frequency, $\mathbf{X}$ and $\mathbf{F}_{\mathrm{b}}$ are the vectors of the Fourier transform of nodal degrees of freedom and of nodal forcing, respectively, and i is the imaginary unit. Here, $\mathbf{M}$, $\mathbf{C}$ and $\mathbf{K}$ are mass, damping and stiffness matrices, respectively, being related to mechanical properties of the vibration system studied, $\mathbf{C}_{\mathrm{Ae}}(\omega)$ is the aerodynamic damping matrix and $\mathbf{K}_{\mathrm{Ae}}(\omega)$ is the aeroelastic stiffness matrix defined in flutter derivatives.

The goal is to develop the frequency-domain model for flutter, vortex-induced and turbulence-induced vibrations of slender plexiglass sheets studied. The aerodynamic input parameters are studied on the section models in the wind canal tests.

3. Generalized analysis of motion

The dynamic displacements of the facade sheets studied are considered as a family of mappings from one region in space and time into another one (see Refs. [1]–[3]). The current configuration is completely defined by the location of displacements in time. The variations of configurations are assumed to be continuous and new boundaries do not appear during deformation. Each new position is defined in relation to a reference position assumed. Adopting the Cartesian coordinates x, y, z and displacements u, v, w, the corresponding Green strain tensor is defined by

$$E_{\mathrm{xx}} = \frac{\partial u_{\mathrm{x}}}{\partial x} + \frac{\left(\dfrac{\partial u_{\mathrm{x}}}{\partial x}\right)^2 + \left(\dfrac{\partial u_{\mathrm{y}}}{\partial y}\right)^2 + \left(\dfrac{\partial u_{\mathrm{z}}}{\partial z}\right)^2}{2}\;,$$

$$Exy = \frac{\dfrac{\partial u_{\mathrm{y}}}{\partial x} + \dfrac{\partial u_{\mathrm{x}}}{\partial y} + \dfrac{\partial u_{\mathrm{x}}}{\partial x}\dfrac{\partial u_{\mathrm{x}}}{\partial y} + \dfrac{\partial u_{\mathrm{y}}}{\partial x}\dfrac{\partial u_{\mathrm{y}}}{\partial y} + \dfrac{\partial u_{\mathrm{z}}}{\partial x}\dfrac{\partial u_{\mathrm{z}}}{\partial y}}{2}\;, \tag{2}$$

$$\text{etc.}$$

In order to establish the constitutive equations with Green strain tensor a stress tensor with the same reference is needed. A symmetric one will be advantageous in present application. The second Piola-Kirchhoff stress tensor denoted as S_{ij} has the desired properties. The equilibrium equation for deformed configuration, stated by the second Piola-Kirchhoff stress tensor, is given by

$$S_{ij} = g(E_{ij})\;, \tag{3}$$

where g is a single valued function of the Green strain tensor E_{ij}.

Considered is the facade shet with volume, surface area and mass density in an initial configuration given by V, S and ϱ_{o}, respectively. The body forces per unit mass are given by $F_{\mathrm{o},i}$ and the surface tractions are specified by the force components T_i.

The facade sheet in equilibrium is subjected to a virtual displacement δu_i being kinematically consistent with the boundary conditions assumed. The balance of virtual work is given by

$$\int S_{ij}\,\delta E_{ij}\,\mathrm{d}V - \int T_i\,\delta u_i\,\mathrm{d}S - \int P_i\,\delta u_i\,\mathrm{d}V = 0 , \tag{4}$$

with

$$P_i = \varrho_{\mathrm{o}}\,F_{\mathrm{o},i} . \tag{5}$$

Equation (4) states that among all kinematically admissible displacement fields u_i the actual one renders the value of the total potential energy stationary.

The incremental form of corresponding variational principle is given by

$$\int S_{ij}^{(1)}\,\delta E_{ij}^{(1)}\,\mathrm{d}V - \int T_i^{(1)}\,\delta u_i^{(1)}\,\mathrm{d}S - \int P_i^{(1)}\,\delta u_i^{(1)}\,\mathrm{d}V = 0 , \tag{6}$$

$$\int S_{ij}^{(2)}\,\delta E_{ij}^{(2)}\,\mathrm{d}V - \int T_i^{(2)}\,\delta u_i^{(2)}\,\mathrm{d}S - \int P_i^{(2)}\,\delta u_i^{(2)}\,\mathrm{d}V = 0 , \tag{7}$$

where superscripts (1) and (2) denote two configurations studied.

The components of surface tractions and body forces refer to the same reference configuration and may therefore be subtracted directly to give

$$\Delta T_i = T_i^{(2)} - T_i^{(1)} , \tag{8}$$

$$\Delta P_i = P_i^{(2)} - P_i^{(1)} . \tag{9}$$

The variations of two displacement fields are chosen to be the same

$$\delta u_i = \delta u_i^{(1)} = \delta u_i^{(2)} . \tag{10}$$

An incremental form of the virtual work equations is then obtained by subtracting Eqs. (6) and (7), giving

$$\int (S_{ij}^{(2)}\,\delta E_{ij}^{(2)} - S_{ij}^{(1)}\,\delta E_{ij}^{(1)})\,\mathrm{d}V - \int \Delta T_i\,\delta u_i\,\mathrm{d}S - \int \Delta P_i\,\delta u_i\,\mathrm{d}V = 0 \tag{11}$$

and considering the virtual variations of both configurations analysed.

When the work done by inertial and damping forces on virtual displacements δu_i is added to Eq. (4), the virtual work principle for the problem studied is given by

$$\int S_{ij}\,\delta E_{ij}\,\mathrm{d}V + \int \varrho\,u_i\,\delta u_i\,\mathrm{d}V + \int C_i\,u_i\,\delta u_i\,\mathrm{d}V - \int T_i\,\delta u_i\,\mathrm{d}S - \int P_i\,\delta u_i\,\mathrm{d}V = 0 , \tag{12}$$

where ϱ and C are mass and damping terms, respectively.

The turbulences in the air flow are described by instantaneous wind speed as function of space and time, with mean and fluctuation components given by

$$u(x, y, z, t) = U(x, y, z) + u'(x, y, z) \; , \tag{13}$$

$$v(x, y, z, t) = V(x, y, z) + v'(x, y, z) \; , \tag{14}$$

$$w(x, y, z, t) = W(x, y, z) + w'(x, y, z) \; . \tag{15}$$

The mean values of U, V, W are the results of averaging of the wind speeds and fluctuating components in a certain time interval.

The turbulence scales of the instantaneous wind speed are the measures of representative dimensions of vortices induced by the turbulences inside of the air flow. They describe the turbulences which 'wrap' the facade sheet in a certain time.

The assessment of such a turbulence motion starts with the specification of the correlation functions of fluctuating components which may be located in longitudinal, transversal and vertical directions. The characteristics of the air flow are well defined if the correlation functions are specified for the mean streamwise components longitudinally and transversally. The correlation in time is specified by formulae

$$\varrho_{u(i)\,u(j)}(\tau) = \frac{R_{u(i)\,u(j)}(\tau)}{\sqrt{(u')^2(t)}\sqrt{(u')^2(t+\tau)}} \; , \tag{16}$$

$$R_{u(i)\,u(j)}(\tau) = u_i(t).u_j(t+\tau) = \lim_{T \to \infty} \frac{1}{T} \int u_i(t).u_j(t+\tau)\,\mathrm{d}t \; . \tag{17}$$

Eq. (17) specifies the covariance function of the process $u(t)$ given by measuring in two space points taking into account the time difference τ (see [4], [5] and [6]).

According to Taylor's hypothesis ([4] the inter-correlation between any of the fluctuating parts, discarding the wind instantaneous speed measured in two points being separated by distance Δx in direction of the wind flow, is equal with the auto-covariance for the period studied. The inter-correlation functions give information concerning the turbulences in direction of the wind action. The existence of the mean values of the wind speed inside of the turbulent flow is given by idiom that in a point i the turbulence has a certain periodicity in time. After a certain period the phenomenon repeats itself in space. These two idioms specify the turbulence scales in time and space. The turbulence scales define the frequency of the wind gusts. The integral length scales correspond to spatial nature of the wind action, specifying the longitudinal, lateral and vertical scales given by

$$L_{\mathrm{x}} = \int \varrho_{u'(i)\,u'(j)}(\Delta x, 0, 0)\,\mathrm{d}(\Delta x) \; , \tag{18}$$

$$L_{\mathrm{y}} = \int \varrho_{u'(i)\,u'(j)}(0, \Delta y, 0)\,\mathrm{d}(\Delta y) \; , \tag{19}$$

$$L_{\mathrm{z}} = \int \varrho_{u'(i)\,u'(j)}(0, 0, \Delta z)\,\mathrm{d}(\Delta z) \tag{20}$$

with integration from 0 until ∞. The most important of these three is the longitudinal scale; the other two are its derivatives. The time scale of turbulence is defined by

$$\Lambda_{\mathrm{T}} = \int \varrho_{u'(i)u'(j)}(\tau)\,\mathrm{d}\tau \; . \tag{21}$$

According to above Taylor's hypothesis, the longitudinal scale of a turbulence may be specified by the time scale and by the mean wind speed V in the streamwise direction given by

$$L_x = V . \Lambda_T \ , \tag{22}$$

The studies for determination of the turbulence scale, both in natural scale and in laboratory, have produced the empirical Davenport's formula

$$\Lambda_T = 0.084 \frac{L}{V} \ , \tag{23}$$

given in sec, where L is the longitudinal scale of the wind speed and V is the mean wind speed.

4. Transient dynamics

The assessment of ultimate structural response is based on the application of updated Lagrangian formulation of motion with reference state taken as current configuration being continuously updated in the deformation process. A new reference frame is established at each stage along updated deformation path of ultimate response. An incremental form of equations of motion is obtained by considering the dynamic equilibrium at two configurations a time step Δt apart. The increments of forcing balance the dynamic equilibrium in time $t + \Delta t$ by

$$\mathbf{M}_t \, \Delta \mathbf{a}_t + \mathbf{C}_t \, \Delta \mathbf{v}_t + \mathbf{K}_t \, \Delta \mathbf{u}_t = \mathbf{R}_{t+\Delta t} - (\mathbf{V}_t^I + \mathbf{V}_t^D + \mathbf{V}_t^S) \ , \tag{24}$$

with inertia forces $\mathbf{V}_t^I = \mathbf{M}_t \, \mathbf{a}_t$, damping forces $\mathbf{V}_t^D = \mathbf{C}_t \, \mathbf{v}_t$, elastic forces $\mathbf{V}_t^S = \mathbf{K}_t \, \mathbf{u}_t$ and with corresponding accelerations, velocities and displacements $\mathbf{a}_t$, $\mathbf{v}_t$ and $\mathbf{u}_t$, respectively. The vectors of nodal point accelerations and velocities are given as time derivatives of the vector of nodal displacements $\mathbf{u}_t$. The mass, damping and stiffness matrices $\mathbf{M}_t$, $\mathbf{C}_t$ and $\mathbf{K}_t$, respectively, are constructed of element matrices established directly. The subscript t denotes the current time and $\mathbf{R}$ is the vector of the wind forcing. If the facade is in equilibrium at time t, the right-hand side of Eq. (24) will be identical with the increment of wind forcing in the time step Δt. The increments in nodal displacements, velocities and accelerations are thus expressed by wind forcing increments and known physical property matrices. If matrices change during time steps then equation (24) is only approximately true. The vector of approximation error given by

$$\Delta \mathbf{V}_{t+\Delta t} = \mathbf{R}_{t+\Delta t} - (\mathbf{V}_{t+\Delta t}^I + \mathbf{V}_{t+\Delta t}^D + \mathbf{V}_{t+\Delta t}^S) \tag{25}$$

is a measure how close to equilibrium the solution has been approached by equation (24).

The governing incremental equation of motion is given in modified Eq. (24) by

$$\mathbf{M}_t \, \Delta \mathbf{a}_t + \mathbf{C}_t \, \Delta \mathbf{v}_t + \mathbf{P}_t \, \Delta \mathbf{u}_t = \Delta \mathbf{R}_t \ , \tag{26}$$

where $\mathbf{P}_t \, \Delta \mathbf{u}_t$ is the vector of nonlinear forces. The pseudo-force method applied here is defined by

$$\mathbf{P}_t \, \Delta \mathbf{u}_t = \mathbf{K}_t \, \Delta \mathbf{u}_t + \mathbf{N}_t \, \Delta \mathbf{u}_t - \Delta \mathbf{V}_{t+\Delta t} \ , \tag{27}$$

where $\mathbf{N}_t \, \Delta \mathbf{u}_t$ is the vector of nonlinear terms (pseudo-forces) and $\Delta \mathbf{V}_{t+\Delta t}$ is approximation error defined above. In the application of the pseudo-force technique the term $\mathbf{P}_t \, \Delta \mathbf{u}_t$ is

placed on the right-hand side of Eq. (26) and the vector of nonlinear terms is treated as pseudo-force vector. At each time step an estimate of $\mathbf{N}_t \Delta \mathbf{u}_t$ is computed and iterations are made until $\Delta \mathbf{V}_{t+\Delta t}$ becomes sufficiently small when compared with tolerance norm adopted. As an estimate for $\mathbf{N}_t \Delta \mathbf{u}_t$ in first iteration at time step Δt, an extrapolated value from previous solutions is used, e.g.

$$\mathbf{N}_t \Delta \mathbf{u}_t = (1 + \alpha) \mathbf{N}_{t-\Delta t} \Delta \mathbf{u}_{t-\Delta t} - \alpha \mathbf{N}_{t-2\Delta t} \Delta \mathbf{u}_{t-2\Delta t} \; , \tag{28}$$

where α is an extrapolation parameter ranging from 0 to 1.

In ultimate analysis it is desirable to seek a strategy of optimal calculations which may be defined in the terms of a number of control parameters specifying the linearization techniques, the frequency of reformulation of effective stiffness matrix, convergence tolerances and limits on the maximum number of iterations and on the degree of variability of time step size adopted.

5. Wave propagation

The wave propagation has two physical aspects – the source of waves and turbulences and the medium where they are running. The source is defined in accordance with laminar and turbulent wind forcing and geometry of the facade sheet studied.

The waves initiated in the source are filtered in the facade sheet and are given by spectral evolution. The diffraction of waves appears in the inhomogeneities of the facade.

The spectral evolution is based on definitions:

1. Each stationary function $x(t)$ is interpreted in integral form by

$$x(t) = \int e^{i \omega t} \, dA(\omega) \; , \tag{29}$$

with $A(\omega)$ as orthogonal complex process.

2. The linear transformation $y(t)$ of the function $x(t)$ in Eq. (29) is given by

$$y(t) = \int H(i \omega) \, e^{i \omega t} \, dA(\omega) \; , \tag{30}$$

with $H(i \omega)$ as the admittance function adopted.

3. Spectral densities of the functions $x(t)$ and $y(t)$ are given by

$$\frac{S_y(\omega)}{S_x(\omega)} = |H(i \omega)|^2 \; . \tag{31}$$

The stationary waves are emitted from the wind forcing with complex amplitude $F(\omega, z_o)$, i.e., $z = z_o$. The wave superposition is given by

$$w_i(t, z) = \int e^{-i \omega t} \, e^{i \, r(\omega z)} \, dF(\omega, z_o) \; . \tag{32}$$

Structural inhomogeneity in the facade is touched by propagating waves. The response spectrum of the inhomogeneity is given by

$$S(\omega, 0) = S(\omega, z_o) \, |H(\omega, 0|^2 \, e^{-2 \, \text{Im}[r(\omega)]} \; , \tag{33}$$

with $H(\omega, 0)$ as structural response due to the wind forcing adopted. The response spectrum is the basis for the number of physical parameters to be specified in the assessment of the facade studied.

6. Linear response

In linear analysis response due to turbulence wind forcing is assumed an arbitrary function of time $b_{\mathrm{F}}(t)$, satisfiyng the Dirichlet conditions together with the condition that $\int |b_{\mathrm{F}}(t)|\,\mathrm{d}t$ is convergent. The equations of the Fourier integral transformation are given by

$$H_{\mathrm{F}}(\omega) = \int b_{\mathrm{F}}(t)\,\mathrm{e}^{-\mathrm{i}\,\omega\,t}\,\mathrm{d}t\ , \tag{34}$$

$$b_{\mathrm{F}}(t) = \frac{1}{2\pi}\int H_{\mathrm{F}}(\omega)\,\mathrm{e}^{\mathrm{i}\,\omega\,t}\,\mathrm{d}\omega\ . \tag{35}$$

For two types of the wind forcing the corresponding transformations $H_{\mathrm{F},1}(\omega)$ and $H_{\mathrm{F},2}(\omega)$ are given by

$$H_{\mathrm{F},1}(\omega) = \int \mathrm{e}^{-a\,t}\,\mathrm{e}^{-\mathrm{i}\,\omega\,t}\,\mathrm{d}t = \frac{1}{a+\mathrm{i}\,\omega}\ , \tag{36}$$

$$H_{\mathrm{F},2}(\omega) = \int \mathrm{e}^{-\mathrm{i}\,\omega\,t}\,\mathrm{d}t = \frac{1-\mathrm{e}^{-\mathrm{i}\,\omega\,t}}{\mathrm{i}\,\omega}\ . \tag{37}$$

The transformations (36) and (37) hold as forcing in the nodes of the facade model adopted. When assuming the operator

$$\mathrm{G} = \partial/\partial t\ , \tag{38}$$

the transformations of inertial forces $-m(z)\,\mathrm{G}^2(u(z,t))$ for above types of forcing are given by

$$\int (-m(z)\,\mathrm{G}^2(u(z,t)))\,\mathrm{e}^{\mathrm{i}\,\omega\,t}\,\mathrm{d}t = m(z)\,\omega^2\,u(z,\omega) + \mathrm{i}\,\omega\,m(z)\,u(z,0) + m(z)\,\mathrm{G}(u(z,0)) \tag{39}$$

with assumption that displacements $u(z,t)$ and their time derivatives $\mathrm{G}(u(z,t))$ obtain zero values for limit $t \to \infty$. The transformation of inertial foces appearing is then given by

$$\int (-m(z)\,\mathrm{G}^2(u(z,t)))\,\mathrm{e}^{\mathrm{i}\,\omega\,t}\,\mathrm{d}t = m(z)\,\omega^2\,u(z,\omega)\ . \tag{40}$$

The algorithm allows the assessment of ultimate facade response in the wind flow.

7. Nonlinear response

In advanced structural dynamics a lot of direct time integration methods exist for numerical analysis of nonlinear time response due to turbulence wind forcing. Explicit, implicit, mixed explicit-implicit, variable and adaptive time integration approaches are employed for a variety of problems appearing.

Explicit methods are represented mostly by the central difference method, with displacements specified in the Taylor series expansion and approximated by second-order accuracy in the development of the time step approaches. They are conditionally stable with second-

order precision in time [7]. Another explicit formulation available is the Modified Euler Method (MEM) presented by Hahn [8]. Tamma [9] and Li [10] developed more efficient explicit, conditionally stable, second-order accurate and direct self-starting formulations in dynamics. The advantages of both direct time integration methods and modal superposition approaches methods combined Tamma in [11] into an explicit, unconditionally stable, second-order accurate VIrtual-Pulse (VIP) time integral method. Another unconditionally stable and second-order accurate explicit algorithm of such type was suggested by Trujillo [12].

Implicit methods require the solution of a set of equations at each time step. Newmark [13] introduced basic implicit algorithm for the time integration problems. The algorithm assumes the constant value of the average acceleration in each integration time step studied. As an implicit scheme the Newmark method is unconditionally stable with the second-order accuracy. As an explicit scheme the Newmark method is only conditionally stable with the second-order accuracy. The Wilson θ-method [14] is essentially an extension of the average acceleration approximation with linear variations between time levels. The collocation methods combine the aspects of the Newmark and Wilson approaches. The collocation approach can be adjusted to reduce either to the Newmark or to the Wilson techniques. The analysis of such approach is submitted in Hilber and Hughes [15]. For the control of the algorithmic damping some modifications have been attempted employing the Newmark family with trapezoidal schemes (see Refs. [16, 17 and 18]).

8. Garbage in, garbage out

Theoretical strategy developed can be interesting, however, the brain washing is an inevitable topic in each aeroelastic analysis. Due to irregularities and turbulences appearing in the air flow and in the inhomogeneities in the facade and its supports, the peril of item 'garbage in, garbage out' appears as significant option in the assessment. Without databank of all experimental results obtained in the wind canal tests, summed up in the corresponding databasis of the problem and being used as input data for calculation, is useless to start the sophisticated analysis in order to obtain the output data required.

The databasis of the problem, obtained by the tests made in the wind canal of The Institute of Structures and Architecture, Slovak Academy of Sciences, Bratislava, with evaluation of the results is partially presented below.

9. Tests in wind canal

The application was made on the plexiglass facade of the famous 'Cheese House', erected in Nitra, Slovakia (Figs. 1 and 2). The facade there was made of yellow plexiglass sheets in order to create the architectural image of the Emmenthaler Cheese.

The facade was connected by joints with supporting steel frame. The width of the plexiglass sheets was 15 mm. The views of the model are in Figs. 3 and 4, with basic dimensions in Fig. 5. The facade acts with wind induced displacements combined with horizontal vibrations of supporting steel structure. The tests were made via strains and accelerations registered in the model of the facade sheet. The location of tensometers is illustrated in Fig. 6. The model was exposed to the wind forcing with velocities 0–40 m/sec. Measured were three accelerations (A1, A2 and A3) and four relative displacements (T1,
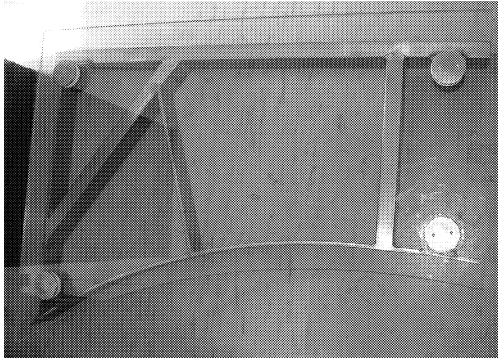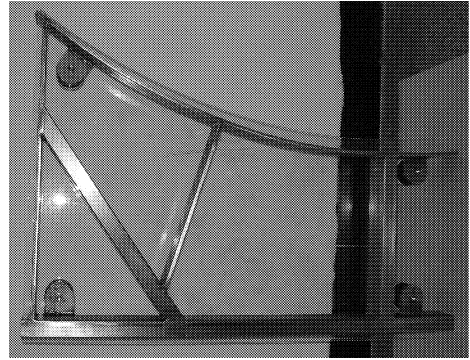
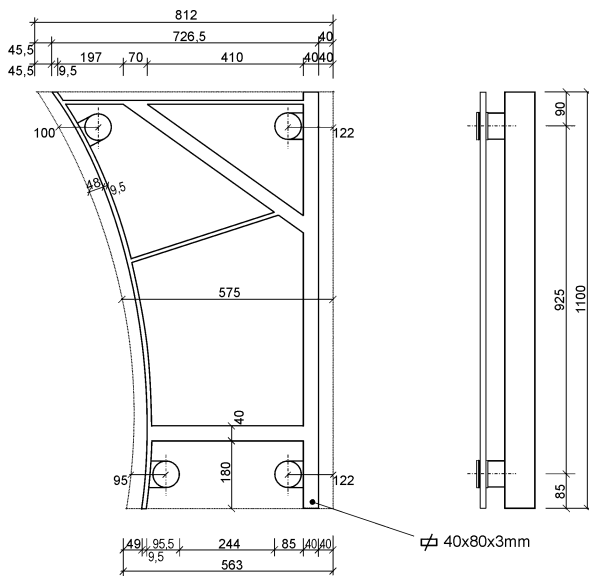Fig.3: View of the model

Fig.4: Another view of the model

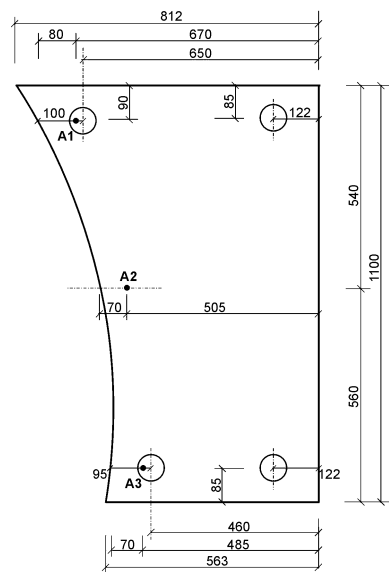Fig.5: Geometry of the experimental set-up
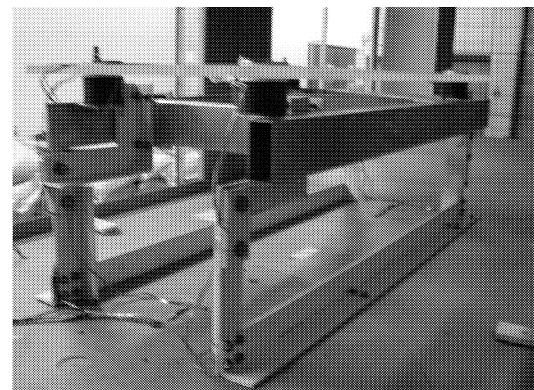

Fig.6: Location of accelerometers

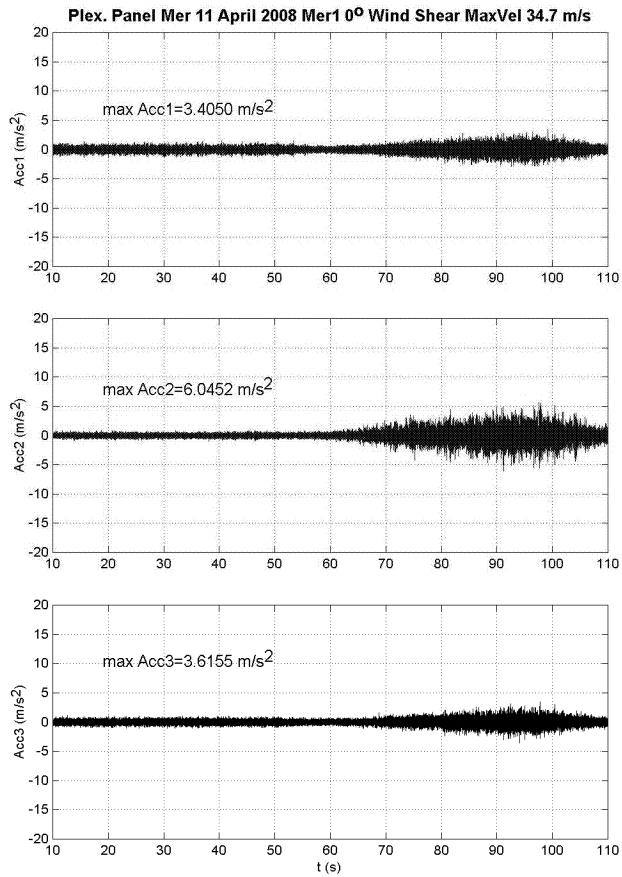Fig.7: Experimental set-up in wind canal for configuration 0°

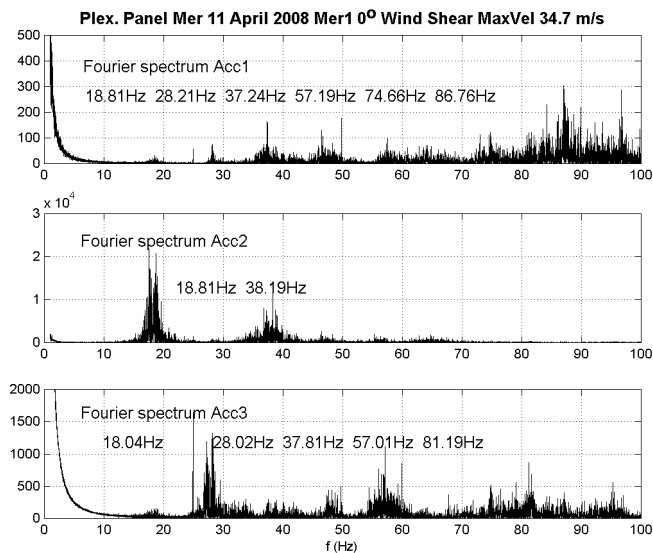Fig.8: Configuration $0°$ – accelerations A1, A2 and A3

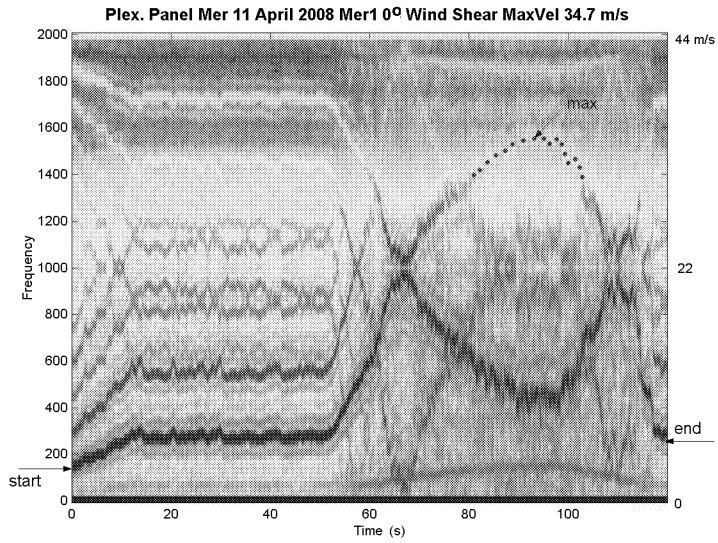Fig.9: Configuration $0°$ – Fourier spectrum of accelerations A1, A2 and A3

Plex. Panel Mer 11 April 2008 Mer1 0⁰ Wind Shear MaxVel 34.7 m/s

Fig.10: Configuration $0°$ – wind velocity Vel (m/s)

Plex. Panel Mer 11 April 2008 Mer1 0⁰ Wind Shear MaxVel 34.7 m/s
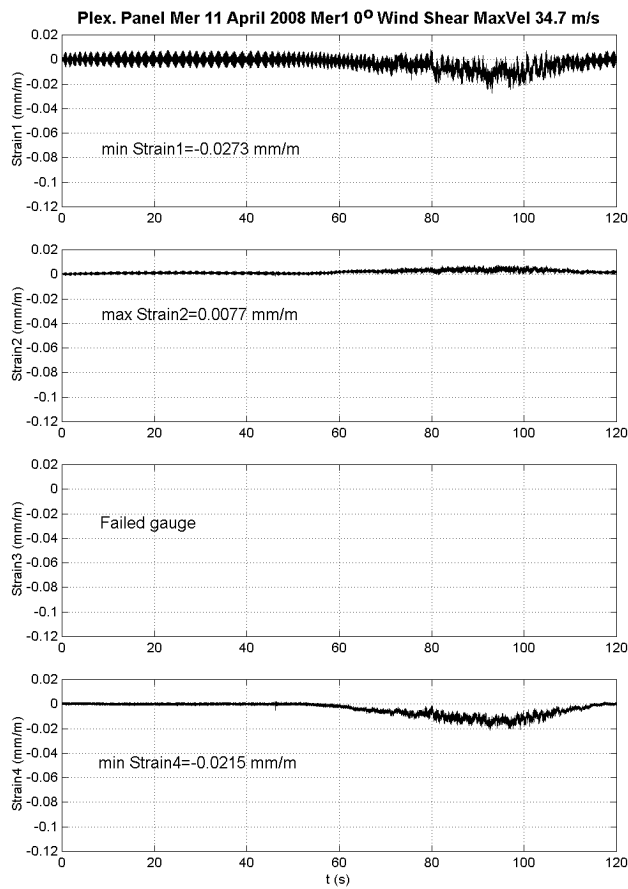
Fig.11: Configuration $0°$ – time response of strains T1, T2, T3 and T4

Plex. Panel Mer 11 April 2008 Mer2 0º Wind Shear MaxVel 36.8 m/s
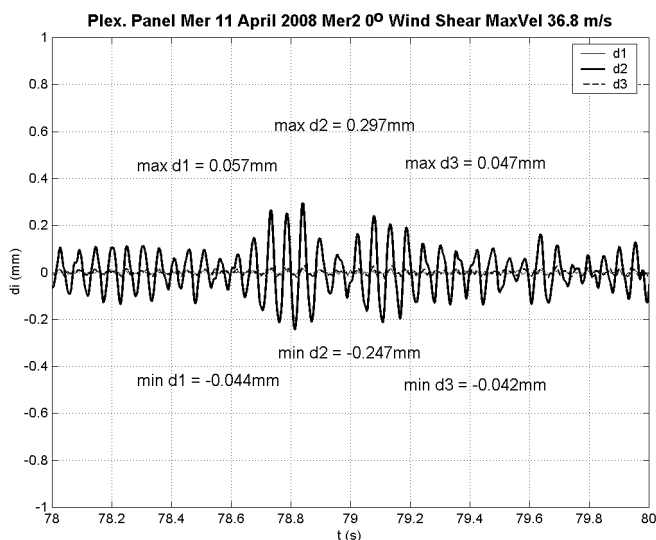
Fig.12: Maximal amplitudes in configuration $0°$ *– Mer 2*

Plex. Panel Mer 15 April 2008 Mer1 -15º Wind Pressure MaxVel 28-40 m/s
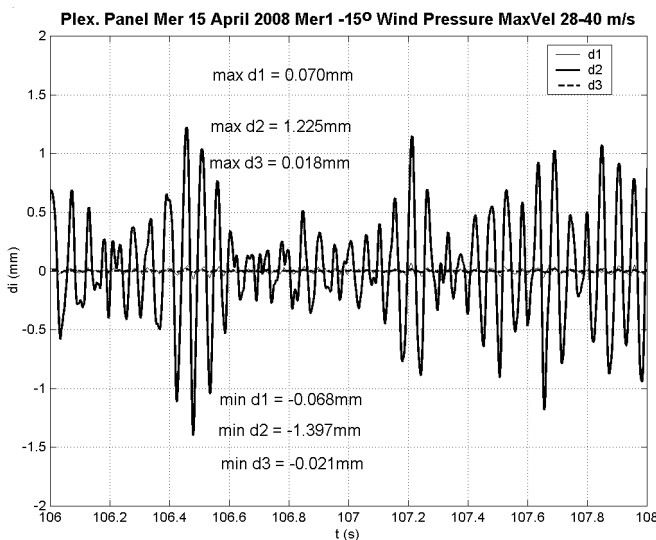

Fig.13: Maximal amplitudes in configuration $-15°$ *– Mer 1*

T2, T3 and T4) under consideration of the air velocity (Vel) in the artificial boundary layer of the wind canal.

Used section of the wind canal had the dimensions $1200{\times}1200$ mm. The testing was made in accordance with the wind loads appearing on the actual facade shet in situ, where the plexiglass sheet is distanced 400 mm from the brick wall of the building. The tests in the wind canal were made for three experimental configurations:

    a) panel in horizontal level $0°$ – shear wind acting parallel along the facade;

    b) panel in skew level $-15°$ – suction due to down wind;

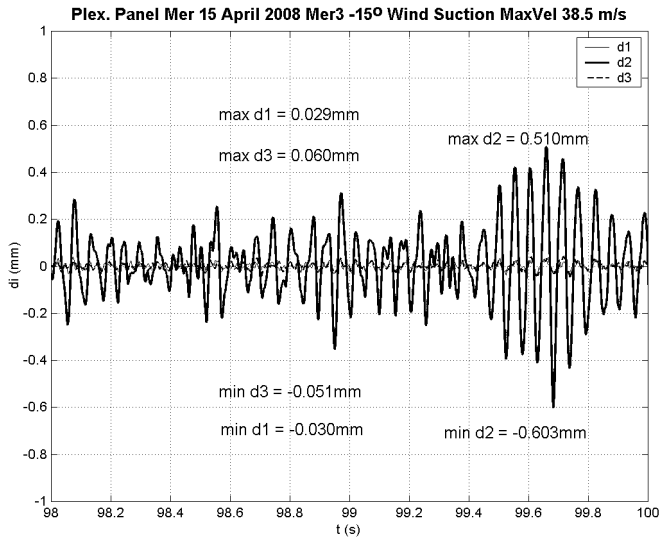   c) panel in skew level $+15°$ – pressure due to skew wind and face uplift wind.
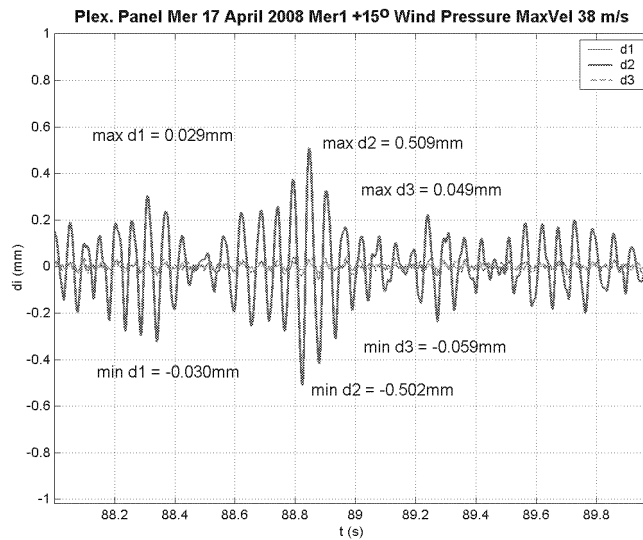
Fig.14: Maximal amplitudes in configuration $-15°$ − Mer 3

Fig.15: Maximal amplitudes in configuration $+15°$ − Mer 1

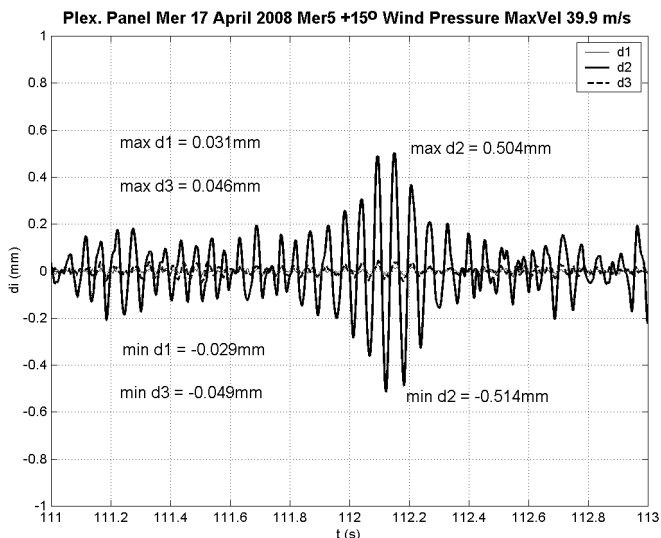| Measurement Nr.	strain T1 ‰	strain T2 ‰	strain T3 ‰	strain T4 ‰
Mer 1	-0.0273	$+0.0077$	–	-0.0215
Mer 2	-0.0223	$+0.0043$	–	-0.0190
Mer 3	-0.0154	-0.0058	–	-0.0108
Mer 4	-0.0269	-0.0077	–	-0.0237
Max. stress	σT1 (MPa)	σT2 (MPa)	σT3 (MPa)	σT4 (MPa)
	-6.9935	-1.9725	–	-6.0713

Tab.1: Max. strains in configuration $0°$

Fig.16: Maximal amplitudes in configuration $+15°$ – Mer 5

Measurement Nr.	strain T1 ‰	strain T2 ‰	strain T3 ‰	strain T4 ‰
Mer 1	-0.1055	0.0178	-0.0207	-0.0659
Mer 2	-0.0757	-0.0409	-0.0137	-0.0471
Mer 3	-0.0777	$-0.0155/+0.0166$	-0.0130	-0.0500
Mer 4	-0.0785	$-0.0195/+0.0106$	-0.0146	-0.0484
Max. stress	σT1 (MPa)	σT2 (MPa)	σT3 (MPa)	σT4 (MPa)
	-27.0262	$4.5599/-10.4775$	-5.3028	-16.8818

Tab.2: Max. strains in configuration $-15°$

Measurement Nr.	strain T1 ‰	strain T2 ‰	strain T3 ‰	strain T4 ‰
Mer 1	$+0.0624$	$+0.0542$	$+0.0210$	$+0.0372$
Mer 2	$+0.0749$	$+0.0363$	$+0.0229$	$+0.0431$
Mer 3	$+0.0716$	$+0.0234$	$+0.0225$	$+0.0419$
Mer 4	$+0.0718$	$+0.0288$	$+0.0230$	$+0.0422$
Mer 5	$+0.0758$	$+0.0319$	$+0.0215$	$+0.0414$
Max. stress	σT1 (MPa)	σT2 (MPa)	σT3 (MPa)	σT4 (MPa)
	$+19.4179$	$+13.8846$	$+5.8920$	$+11.0411$

Tab.3: Max. strains in configuration $+15°$

The results obtained for configuration a) are illustrated in Figs. 7–11. The out of plane amplitudes of vibration in all three configurations are plotted in Figs. 12–16. The displacements out of the plane of the panel have dominant frequency 18.2–18.3 Hz. The evaluation of the results obtained is made in Tables 1, 2 and 3. The comparison of experimental and numerical results obtained is summed up in Tables 4, 5 and 6. In accordance with time response and extremal values of the data in above figures and tables, the resultig response of the facade sheet is dominated by dynamic displacements with pressure and sucking of the wind. The displacements have irregular distribution along the surface with turbulences distinctly influencing the deformations and vibrations of the facade shet studied.

Measurement Nr.	max. wind velocity (m/s)	acceleration A1 (m/s^2)	acceleration A2 (m/s^2)	acceleration A3 (m/s^2)
Mer 1	34.7	3.405 (3.353)	6.045 (6.212)	3.616 (3.741)
Mer 2	36.8	3.319 (3.289)	7.235 (7.342)	3.327 (3.793)
Mer 3	26.4	1.760 (1.732)	3.080 (3.127)	2.065 (2.211)
Mer 4	36.3	3.664 (3.613)	7.527 (7.755)	3.766 (3.835)
Extreme displacements in Mer 2		d1 (mm)	d2 (mm)	d3 (mm)
min		−0.044 (−0.047)	−0.247 (−0259)	−0.042 (−0.049)
max		+0.057 (+0.062)	+0.297 (+0.311)	+0.047 (0.052)

Tab.4: Max. accelerations in configuration $0°$, measured and (calculated)

Measurement Nr.	max. wind velocity (m/s)	acceleration A1 (m/s^2)	acceleration A2 (m/s^2)	acceleration A3 (m/s^2)
Mer 1	28.40	8.880 (8.920)	12.421 (12.567)	2.365 (2.513)
Mer 2	37.20	5.367 (5.375)	13.622 (13.736)	4.939 (5.067)
Mer 3	38.50	7.062 (7.088)	15.227 (15.562)	6.059 (6.214)
Mer 4	38.30	6.464 (6.598)	14.599 (14.952)	7.050 (7.146)
Extreme displacements in Mer 1		d1 (mm)	d2 (mm)	d3 (mm)
min		−0.068 (−0.072)	−1.392 (−1.422)	−0.021 (−0.028)
max		+0.070 (+0.079)	+1.225 (+1.341)	+0.018 (+0.019)

Tab.5: Max. accelerations in configuration $-15°$, measured and (calculated)

Measurement Nr.	max. wind velocity (m/s)	acceleration A1 (m/s^2)	acceleration A2 (m/s^2)	acceleration A3 (m/s^2)
Mer 1	38.00	6.628 (6.702)	10.519 (10.531)	5.424 (5.582)
Mer 2	38.60	6.533 (6.551)	10.021 (19.049)	5.432 (5.593)
Mer 3	38.50	6.381 (6.395)	10.354 (10.367)	6.085 (6.123)
Mer 4	38.80	6.063 (6.095)	9.997 (10.212)	4.942 (4.972)
Mer 5	39.90	5.639 (5.646)	12.365 (12.877)	5.605 (5.827)
Extreme displacements in Mer 5		d1 (mm)	d2 (mm)	d3 (mm)
min		−0.029 (−0.033)	−0.514 (−0.538)	−0.049 (−0.53)
max		+0.031 (+0.035)	+0.504 (+0.539)	+0.046 (+0.051)

Tab.6: Max. accelerations in configuration $+15°$, measured and (calculated)

The results obtained were summed up in the databasis of input data for the wind resistant design of the plexiglass facade suggested.

10. Conclusions

The results submit some image on ultimate aeroelastic behaviour of facades made of plexiglass sheets. The approaches suggested allow the aeroelastic assessment of the problem. Established was the databasis of evaluated experimental results. Such databasis obtained by the tests made in the wind canal contains all input data for numerical analysis and for the development of virtual models for the assessment of aeroelastic reliability of such structures.

On the basis of the evaluation of the results obtained was made the design of the plexiglass facade with satisfaction of all safety and reliability requirements and with following succesful in situ implementation.

References

 [1] Tesar A.: Aeroelastic Response of Transporter Shell Bridges in Smooth Air Flow, Norwegian Institute of Technology, Tapir, Trondheim, 1978
 [2] Tesar A.: Transfer Matrix Method, KLUWER Academic Publishers, Dordrecht/Boston/London, 1988
 [3] Tesar A., Svolik J.: Wave distribution in fibre members subjected to kinematic forcing, Int. Journal for Communication in Numerical Mechanics, 9, 1993
 [4] Hautoy C.: Simulation des proprietes dynamiques du vent, Souflerie a couche limite du C.S.T.B., Nantes, France, 1990
 [5] Moonen P., Blocken B., Carmeliet, J.: Indicators for the evaluation of wind tunnel test section flow quality and application to a numerical closed circuit wind tunnel, J.W.E.I.A., (95), pp. 1289–1314 (2007)
 [6] Teleman E.C., Silion R., Axinte E., Pescaru R.: Turbulence scales simulations in atmospheric boundary layer wind tunnels. Bulletinul Institutului Polytehnic din Iasi, Publicat de Universitatea Tehnica 'Gheorghe Asachi' din Iasi, Tomul LIV (LVIII), Fasc. 2, 2008, pp. 7–14
 [7] Krieg R.D.: Unconditional Stability of Numerical Time Integration Methods, Journal of Applied Mechanics, 1973, 40, 417
 [8] Hahn G.D.: A Modified Euler Method for Dynamic Analysis, International Journal for Numerical Methods in Engineering, 32, 1991
 [9] Tamma K.K., Namburu R.R.: A Robust Self-Starting Explicit Computational Methodology for Structural Dynamic Applications : Architecture and Representations, International Journal for Numerical Methods in Engineering, 29, 1990
[10] Li M., Tamma K.K., Namburu R.R.: Evaluation and Applicability of Explicit Self-Starting Formulations for Nonlinear Structural Dynamics, AIAA SDM Conference, San Diego, CA, April, 1991
[11] Tamma K.K., Mei Y., Chen X., Sha D.: Recent Advances Towards an Effective Virtual-Pulse (VIP) Explicit Time Integral Methodology For Multidimensional Thermal Analysis, International Journal of Numerical Methods in Fluids, 20, 1995
[12] Trujillo D.M.: An Unconditionally Stable Explicit Algorithm for Structural Dynamics. International Journal for Numerical Methods in Engineering, 11, 1977
[13] Newmark N.M.: A Method of Computation for Structural Dynamics. ASCE Journal of the Engineering Mechanics Division, Vol. 85, No. EM3, 1959
[14] Wilson E.L.: Dynamic Response by Step-By-Step Matrix Analysis, Proceedings, Symposium On The Use of Computers in Civil Engineering. Laboratorio Nacional de Engenharia Civil, Lisbon, Portugal, October 1–5, 1962
[15] Hilber H.M., Hughes T.J.R.: Collocation, Dissipation and Overshoot for Time Integration Schemes in Structural Dynamics, Earthquake Engineering and Structural Dynamics, 6, 99, 1978
[16] Hilber H.M., Hughes T.J.R., Taylor R.L.: Improved Numerical Dissipation for Time Integration Algorithms in Structural Dynamics, Earthquake Engineering and Structural Dynamics, 5, 1977
[17] Hoff C., Pahl P.J.: Development of an Implicit Method with Numerical Dissipation from a Generalized Single Step Algorithm for Structural Dynamics, Computer Methods Appl. Mech. Eng., 67, 1988
[18] Wood W.L., Bossak M., Zienkiewicz O.C.: An Alpha Modification of Newmark's Method. International Journal for Numerical Methods in Engineering, 15, 1980